VULNERABILITY MAPPING AND PROTECTION ZONING OF KARST SPRINGS. VALIDATION BY MULTITRACER TESTS

Marín A.I.*, Andreo B., Mudarra M.

Department of Geology and Centre of Hydrogeology University of Málaga (CEHIUMA), 29071 Málaga, Spain

****Corresponding author**: *aimarin@uma.es +34 951 952997*

Abstract

Protection zoning of karst springs and wells used for water supply is a key aspect in many countries, calling for specific methodologies adapted to the particular characteristics of karst media. This work presents a new approach, in view of the present state of the art and based on experiences with contamination vulnerability mapping at the pilot site of the Villanueva del Rosario karst system (southern Spain). Source (intrinsic) vulnerability maps were prepared and compared using three European procedures for karst aquifers. The vulnerability maps were then tested using dye tracers. The COP+K method and Slovene Approach appear to provide reliable results in terms of intrinsic vulnerability mapping. Nevertheless, all the methods have a margin of error. The COP+K map is adopted as the baseline to delineate the protection zones, through the conversion from vulnerability classes to degrees of protection.

Keywords: *groundwater protection, protection zoning, tracer test, karst, Spain*

1. Introduction

Delineating protection zones for water supply and implementing proper land-use practices in surrounding areas are crucial aspects for a sustainable use of valuable drinking water resources (Adams and Foster, 1992; Foster at al., 2013). To prevent groundwater pollution, mostly owing to human activity, it is necessary to find a balance between socio-economic development and reasonable land-use planning.

According to Guidance Document No. 16 of the Water Framework Directive (WFD) on groundwater (European Commission, 2007), addressing Drinking Water Protected Areas (DWPAs) defined under Article 7 (European Commission 2000), protection measures should be

focused on (but not necessarily restricted to) zones around current or planned abstractions (safeguard zones or protection zones) in order to comply with Article 7 and Article 4.2.

In the context of delineating protection perimeters for groundwater sources for human supply, policy and standards vary from country to country (SAEFL, 2004; DVGW, 2006; DELG-EPAGS, 1999). This disparity is reflected in the number of zones established, the requirements concerning minimum dimensions, and the regulations regarding potentially polluting land-use activities. Yet vulnerability mapping, together with travel-time methods, is already used in many Member States as the approach for delimiting safeguard zones (European Commission, 2007)

In Europe, carbonate terrains occupy 35% of the land surface, and contribute up to 50% of the drinking water in some countries (European Commission, 1995). Freshwater from karst springs is a very important renewable natural resource. One obvious way of wasting this resource is through groundwater contamination. Karst aquifers are particularly sensitive to contamination, having a very low self-cleaning capacity due to their structure and hydrological behaviour (Ford and Williams, 1989; Dörfliger and Zwahlen, 1997; Zwahlen, 2004), the flow concentration in the epikarst, a rapid recharge of infiltrating water underground and its fast distribution over large distances, high flow velocities and short residence time, etc. Consequently, the methodologies applied to delineate protection zones in karst aquifers call for additional, more specific considerations (Dörfliger and Zwahlen, 1997; Zwahlen, 2004, European Commission, 2007; Goldscheider, 2010). In acknowledgement of these issues, the Directorate General for Science, Research and Development of the European Commission supported the COST Action 620: “Vulnerability and Risk Mapping for the Protection of Carbonate (Karst) Aquifers”.

Following official guidance documents on groundwater in drinking water protected areas (European Commission, 2007), the protection zones in karst aquifers may need to be defined using vulnerability maps as the tool

The concept of vulnerability to contamination has been defined and developed by many researchers (Margat, 1968; Foster, 1987; Zaporozec, 1994; among others). European COST Action 620 (Zwahlen, 2004) aimed for consensual guidance about vulnerability and risk mapping for the protection of karst aquifers. Accordingly, ‘intrinsic vulnerability’ was described as the sensitivity to contamination of an aquifer, taking into account its geological, hydrological and hydrogeological characteristics, regardless of the nature and scenario of the contamination.

A European Approach was proposed within the COST Action framework for groundwater vulnerability mapping: the origin-pathway-target model (Daly et al. 2002), which discerns resource and source vulnerabilities, depending on the target or the receptor of potential contamination. In the case of resource vulnerability, the target to protect is the top of the saturated zone; the pathway is mainly through the layers above the groundwater surface. For source vulnerability assessment, in turn, the target is the karst water supply (borehole or spring), and consequently the pathway should include the unsaturated and saturated zones. The two concepts are very closely related, as it is impossible to protect a source without protecting the resource.

Several methodologies to assess vulnerability to pollution in karst aquifers have been evolved over the past two decades. Based on COST Action 620 recommendations and EPIK, the first method specifically designed for karst vulnerability mapping, Dörfliger and Zwahlen, 1997), many other methods for vulnerability assessing and mapping have been developed. They include PI (Goldscheider et al., 2000), KARSTIC (Davis et al. 2002); COP and COP+K methods (Vías et al., 2006, Andreo et al. 2009), the Slovene Approach (Ravbar and Goldscheider, 2007), or PaPRIKa (Kavouri et al., 2011). Geographic information systems and GIS-based approaches are widely used for the intrinsic vulnerability mapping of karst aquifers, although there are also relevant advances in geological and hydrogeological modelling for karst systems (Jeannin et al., 2013; Hartman et al., 2014; Turk et al., 2014).

Groundwater contamination vulnerability mapping has implicit weaknesses, most notably residing in the subjectivity of its application. Nevertheless, it remains a tool with great potential for groundwater quality protection. It is relatively simple to apply, if supported by appropriate hydrogeological studies and baseline maps, and its implementation within land-use planning policies is intuitive, as the outcome is a map that shares a common territorial basis with the working environment.

The main aim of this work is to propose an approach for protection zoning karst springs based on the application and the comparison of results from contamination vulnerability methods, with validation of results by dye and natural tracers.

Despite increasing scientific contributions in terms of vulnerability mapping and groundwater protection, even in karst aquifers, there is still a need for new ideas, methods and strategies

when facing the practical challenges of karst spring protection. The present work provides orientation in delineating protection zones for public drinking-water supplies in karst Drinking Water Protected Areas. The approach described here may serve to control diffuse pollution and prevent further deterioration of the environment (Water Framework Directive Guidance Document No. 16; Nitrates Council Directive 91/676/EEC; COST Action 620, European Commission, 1991). In view of the European guidelines for the protection of karst groundwater, the present proposal involves the application of pollution vulnerability assessment as a referential map to delineate protection zones. To this end, three methods for source vulnerability mapping were applied and compared, not only resource vulnerability maps, as in majority of previous studies (Vías et al., 2005; Neukum and Hötzl, 2007; Marín et al., 2012). As the final step, this work highlights the need to validate results obtained in karst aquifers where high anisotropy and heterogeneity can limit the extrapolation of data. Vulnerability maps and protection zoning should be validated to ensure their adequacy for land use management and groundwater protection (Andreo et al., 2006; Goldscheider, 2010). Validation may involve a wide range of methods and techniques (dye tests, natural responses of springs, environmental tracers, etc.), allowing for the characterization of fast and slow flows within the system, aquifer responses for high and low water conditions, the global response of the system, or the response to any short-term signal. The present study applies artificial dye tracers specifically tested for the identification of recharge areas and flow velocities, to assess and validate pollution vulnerability maps (Käss, 1998; Andreo et al., 2006; Benischke et al., 2007; Goldscheider, 2008; among others).

2. Pilot site: background and previous works

The case study is the catchment area of Villanueva del Rosario spring (14 km^2), largely responsible for drainage of the Sierra Camarolos and Sierra del Jobo aquifer (28 km^2), located 30 km north of the city of Malaga, Southern Spain (Fig. 1). The relief is rugged, with altitudes ranging from 600 to 1,640 m a.s.l. The climate is temperate Mediterranean, with a mean historic annual precipitation of 760 mm, highly influenced by the altitude (below 600 mm in the lower sectors and up to 900 mm in the higher areas). The precipitation regime is associated with wet winds coming from the Atlantic Ocean in autumn, winter and, to a lesser extent, in springtime. The mean annual temperature is around 14°C, but there are only temperature records for lower

121 areas of the aquifer. The prevailing vegetation is Mediterranean scrubland with forest patches
122 (Mediterranean forest and pines from reforestation).
123 Geologically, the test site is situated within the Betic Cordillera and is made up of Jurassic
124 carbonate rocks, with a maximum total thickness of 400-450 m (Peyre, 1974). The base of the
125 stratigraphic series is constituted by Upper Triassic clays with evaporite rocks (mainly gypsum).
126 Above these lies a dolomite formation followed by limestones; at the top, there are Cretaceous-
127 Paleogene marly-limestones and marls. To the north and south of Alta Cadena, Flysch-type
128 rocks crop out, including Tertiary clays and sandstones. The geological structure of the aquifer
129 is characterized by a severe degree of deformation: ENE–WSW lying folds, from which
130 overthrusts developed, with S–SE vergence (Figs. 1 and 2). The whole structure is affected by
131 more recent fractures (faults and joints) in a mainly NW–SE direction (Figs. 1 and 2; Martín-
132 Algarra 1987). This geological complexity causes hydrogeological heterogeneity.
133 Two main soil types can be distinguished. The carbonate outcrops are covered by patchy
134 leptosols (thickness < 30 cm), whereas less permeable soils with a thickness of 10–70 cm and a
135 silty–clayey texture overlie the Cretaceous marls.
136 Karst features are developed mainly on Jurassic limestones, with large karrenfields, dolines and
137 uvalas. There are also some karst swallow holes (Fig. 1) which become active during storms or
138 heavy rainfall. No evidence of caves exists in the study area, despite the activity of speleological
139 groups.
140 From a hydrogeological standpoint, the aquifer is constituted by fractured and karstified Jurassic
141 carbonate rocks, limited along almost all their borders of a tectonic nature by low permeability
142 materials (Triassic and Flysch clays and Cretaceous-Paleogene marls). The boundaries and
143 recharge area of the system were outlined taking into account the results obtained from
144 hydrogeological studies and multitracer tests (Mudarra et al., 2010; Mudarra et al., 2014a). On
145 5th February 2009, an initial multitracer test was performed in the aquifer under very high water
146 conditions (2,445 l/s of spring outflow), coinciding with heavy rainfall conditions (67 mm/d) as
147 part of a rainy period (194 mm from January 31 to February 6); this fed the existence of surface
148 runoff into two karst sinkholes, where uranine and eosin were injected (P-1 and P-2 respectively
149 in Fig. 1). Details on the methodological procedure and results can be found in Mudarra et al.
150 (2010, 2014a). Both dyes were detected only at Villanueva del Rosario spring and in an

151 associated overflow spring. Briefly, the first dye tracer detected in the spring water was eosin,
152 17 h after injection, with a maximum concentration of 3.29 µg/l recorded 22.5 h after injection.
153 The uranine was detected 27 h after injection, its peak concentration of 19.10 µg/l reached at
154 30.5 h after injection. The peak flow velocities recorded in this test for eosin and uranine were
155 145 and 215 m/h, respectively. The recovery rates of the two dyes were 21% (420 g) for eosin
156 and 71% (2,130 g) for uranine. The main purpose of this test was to define groundwater
157 connections and flow velocities and to delimitate the catchment area of Villanueva del Rosario
158 spring.
159 Recharge of the system takes place entirely by rainfall water, whether concentrated (via
160 swallow holes) or diffuse. The groundwater flow paths are predominantly NE-SW and S-N.
161 Discharge occurs naturally toward the northern border of the carbonate outcrops, toward the
162 Villanueva del Rosario spring (770 m a.s.l.), whose water is mainly used for the drinking supply
163 of Villanueva del Rosario village, but there are no human settlements above the aquifer.
164 This spring (260 l/s historic annual mean outflow) responds rapidly to precipitation events (Fig.
165 3), with sharp, significant increases in discharge rates (several per hydrological year), which are
166 proportional to the quantity and intensity of rainfalls. Moreover, flow velocities (exceeding 200
167 m/h) prove the high degree of functional karstification within the aquifer sector drained by
168 Villanueva del Rosario spring (conduit flow system), whose connection with swallow holes has
169 been verified by means of the above-mentioned tracer test (Mudarra et al., 2010, 2014a). These
170 results are coherent with information provided by natural tracers of infiltration (Total Organic
171 Carbon, Cl^- and NO_3^- contents, intrinsic fluorescence values related to soil fulvic and humic
172 acids), which showed increases (or drops in the case of Cl^- and NO_3^-) in every recharge event
173 (coinciding with the lowest values for water mineralization), with response times around 1 day
174 (Mudarra and Andreo, 2011, Mudarra et al., 2011, 2014b).
175 In the study area, there are few potential sources of water contamination. Scattered livestock
176 farming activity takes place above the carbonate outcrops, concentrated in slightly endorrheic
177 areas of shallow slopes.
178

3. Methodologies

3.1. Source vulnerability mapping

The objective of contamination vulnerability mapping is to identify the most vulnerable zones in catchment areas and to provide criteria for protecting the groundwater used for drinking water supply (Foster et al., 2013).

Three approaches for source vulnerability mapping were applied to assess the vulnerability to pollution of the pilot site selected for this work: the COP+K method (Vías et al., 2006; Andreo et al., 2009), the Slovene Approach (Ravbar and Goldscheider, 2007) and the PaPRIKa method (Kavouri et al., 2011). These methods are specific for karst aquifers, while the variables, parameters and factors were established in view of the European Approach arising from Action COST 620 (Daly et al., 2002; Zwahlen, 2004). The methods account for the properties of any overlying layers in terms of advective transport times and physical attenuation, assessing the relative protective function of the different layers between the land surface and groundwater; variables related to flow concentration (karst features, slopes, etc); and others associated with the groundwater flow within the saturated zone. The precipitation variables are considered under the COP and Slovene Approach, but not for the PaPRIKa method.

Approaches applied to vulnerability mapping make it possible to assess the resource vulnerability to pollution as the baseline; but they lead to source vulnerability maps by adding considerations about flow within the saturated zone (K factor for COP and Slovene approach, or I_{source} for PaPRIKa method; see Vías et al., 2006; Andreo et al., 2009; Ravbar and Goldscheider, 2007; Kavouri et al., 2011). The Slovene Approach is based on COP yet adapted to the Slovene environment; both methods use the same variables (travel time, karst network and connection) to evaluate groundwater flow within the saturated zone, and derive to source vulnerability maps from resource vulnerability maps. However, the Slovene Approach is more restrictive regarding the assignment of the highest source vulnerability class (Andreo et al., 2009).

To obtain a source vulnerability map by means of PaPRIKa, the I factor (corresponding to the C factor of the European approach) is changed to I_{source} factor by the addition of transit time isochrones defined from the source, dividing the study area into two: inside or outside the isochron (see Kavouri et al., 2011).

209 Table 1 summarizes the characteristics of the unsaturated and saturated zones, the aquifer
210 structure and its hydrological behaviour, as considered by the methods applied.

211 **Table 1** Variables considered by the selected methods for vulnerability mapping

Variables	Methods COP	Slovene Approach	PaPRIKa
Karst unsaturated zone			
Topsoil thickness	**x**	**x**	**x**
Topsoil texture	**x**	**x**	**x**
Topsoil structure (stoniness)			**x**
Subsoil permeability	**x**	**x**	**x**
Subsoil thickness		**x**	**x**
Permeability	**x**	**x**	**x**
Confined condition	**x**	**x**	
Depth of the unsaturated zone	**x**	**x**	**x**
Fracturing	**x**	**x**	**x**
Epikarst aquifer			**x**
Recharge conditions			
Concentrated flow	**x**	**x**	**x**
Temporal variability		**x**	
Slope gradient	**x**	**x**	**x**
Vegetation cover	**x**	**x**	
Karst landforms	**x**	**x**	**x**
Precipitation	**x**	**x**	
Karst saturated zone			
Hydrogeological behavior	**x**	**x**	**x**
Tracer test interpretation	**x**	**x**	**x**

212

3.2. Tracer experiment characteristics

From 2nd May to 11st May 2011, a new tracer test was carried out, this time under moderate-high hydrodynamic conditions (1,208 l/s of maximum spring outflow, Fig. 3) in order to check vulnerability mapping and protection zoning. Four points with different landform characteristics were selected for simultaneous dye injections in the catchment area of Villanueva del Rosario spring (Figs. 4 and table 2). Then, 2 kg of uranine (Acid yellow 73, CAS: 518-47-8) was directly poured over calcareous breccia outcrops located at 1,356 m a.s.l. (P 3, Fig. 4); 2 kg of Sulforhodamine-B (Acid red 52, CAS: 3520-42-1) was discharged at point P-4 (Fig. 4), over a highly developed karrenfield where water runoff from impervious outcrops infiltrates; and 2 kg of eosin (Acid red 87, CAS: 17372-87-1) was directly poured on a moderately developed karrenfield NE of Chamizo peak (P-5 in Fig. 4). Finally, 2 kg of pyranine (Solvent green 7, CAS: 63358-69-6) was injected in a swallow hole located South of Cortijo del Jobo (P-1 in Figs. 1 and 4). All substances were transported as a powder to selected points, where they were diluted previous to injection, using a variable volume of rainfall water (eosin and uranine) or runoff water (sulforhodamine-B and pyranine). Injections ended when all dyes were dissolved and poured into the points, an interval lasting under 20 minutes. The end hour of injection is noted in Table 2.

At Villanueva del Rosario spring (and its associated overflow spring, which was active for two days), 131 water samples were manually collected in 60 ml dark glass bottles, with increasing periodicity from 1 to 12 hours, for subsequent dye determination in the laboratory of the Centre of Hydrogeology of University of Malaga (Perkin-Elmer LS55 spectrofluorometer, synchronous-scan-procedure). Water samples were transported and stored in darkness, preventing tracer photodegradation and microbial activity, causative processes of reduction of fluorescent tracer concentration in the water. Sample analyses were performed within 48 hours. Analytical detection limits for dyes were 0.04 µg/l (uranine), 0.3 µg/l (eosin), 0.5 µg/l (sulforhodamine-B and pyranine). On 4th May, a field spectrofluorometer (GGUN- FL30, Albillia, Switzerland) was installed at the main spring, in order to achieve a continuous record (every 10 minutes) of concentrations of 3 of the 4 injected tracers (except pyranine, due to a technical limitation). Field spectrofluorometer were logged until 23rd November 2011.

Other possible discharge points were monitored but no tracers were detected in water.

243

244

245 **Table 2** Main characteristics of injection points for the multitracer test of May 2011 (see location in Fig. 4)

Characteristics	**P-3**	**P-4**	**P-5**	**P-1**
Dye tracer	Uranine	Sulforhodamine B	Eosin	Pyranine
Altitude (m a.s.l.)	1356	1280	1224	1145
Distance (m)[1]	2930	2810	5900	6600
Soil depth	Patches (< 10 cm)	< 30 cm	Patches (< 20 cm)	> 75cm
Lithology	Calcareous breccias	Limestones	Limestones	Limestones
Karst landscape	Karren scarcely developed	Karren with additional recharge from runoff	Karren	Swallow hole
End of injection	10:30	8:45	7:45	8:35
Detection at the spring	No	Yes	No	Yes
[1] Distance from injection point to Villanueva del Rosario spring				

246

247 **4. Proposal for protection zoning**

248 Following the WFD and other guidance/recommendation documents, the definition of protection
249 zones of drinking water supply in karst aquifers is based on the source (spring or well)
250 vulnerability maps. The entire catchment of a spring would need to be integrated within
251 protection zones due to the high heterogeneity and uncertainty in extrapolation processes when
252 dealing with karst aquifers. The GIS-based methods lead to fuzzy spatial distributions of
253 vulnerability classes. The vulnerability map should be smoothed (giving priority to environmental
254 protection) before changing the focus to protection zones, looking for the usefulness for
255 implementation in land-use planning. Thus, establishing the source vulnerability map as the
256 main criterion, three different types of source protection zones are proposed in this work. They
257 could be adapted to national legislations.

- Zone I, which requires high protection, comprising zones with higher source vulnerability. The pollutant could rapidly reach the water supply point, hence land-use restrictions should be strict. Activities that could reduce the natural aquifer protection (removing soil layers or changing the unsaturated thickness) or become a pollution source (hazard) require special vigilance.
- Zone II, where moderate protection is needed. The source vulnerability to contamination is moderate. In this area it is possible to develop human activities without direct impact on the spring, which is consistent with a certain self-cleaning capacity of the aquifer.
- Zone III requires low protection. It includes the sector of the aquifer where the vulnerability to contamination is low. The land-use restrictions are lesser than in the other two zones.

Once the protection zones are defined, the respective management agency should set specific criteria for the land-use activities in the catchment area of the spring/well, according to the gradation of perimeter protection, and enforce them. This calls for detailed studies to analyse the characteristics of permitted activities in order to minimize the risk situations. Figure 5 shows the implementation schema for land-use management of groundwater drinking water supply protection zones that is proposed in this work. Based on pollution vulnerability assessment (source vulnerability), the vulnerability classes are converted into protection zones, according to the criteria exposed in this work or following national legislation. The perimeter protection levels are then derived from the direct conversion of vulnerability categories into protection zones. The inventory and location of human activities that pose a threat to groundwater quality and land-use management policies are the next step, needed to determine the activity suitability with respect to the degree of protection. Monitoring and security measures would be implemented to ensure that water abstraction activity is not affected. Therefore, the limits of the protection perimeter and the zones established should be periodically reviewed to adapt them, if necessary, to newly arising factors or to new hydrogeological knowledge.

286 ## 5. Results

287 ### 5.1. Source vulnerability mapping

288 Three methods exposed previously for source vulnerability mapping (section 3.1) were applied
289 in the Villanueva del Rosario catchment area. In this work, the assessment of the factors related
290 to groundwater flow within the saturated zone (K factor or I_{source}) was done using the
291 experimental results of tracer tests (two dyes injected) carried out in 2009 (Mudarra et al., 2010,
292 2014a; see section 2). These data served as the basis to assess travel time (t), active conduit
293 network (n) and contribution or connection (r) considered in the K factor, according to Andreo et
294 al. (2009), for COP+K method and Slovene approach; and to define the isochrones for the
295 PaPRIKa method (Kavouri et al., 2011).
296 The methods COP+K and Slovene approach estimate the vulnerability value by means of a
297 mandatory algorithm. However, assessment by PaPRIKa allows for the selection of weighting
298 values based on personal experience and judgment by hydrogeologists. Here, several
299 weighting combinations were tested. The retained combination was 0.4I+0.2P+0.2R+0.2Ka, as
300 it provided higher vulnerability for swallow holes areas and was also the option most often
301 selected for the other test sites where the PaPRIKa method was standardized (Dörfliger and
302 Plagnes, 2009).
303 Figure 6 shows the source vulnerability maps of Villanueva del Rosario spring resulting from
304 application of the three methods. Comparative analysis shows that the spring vulnerability
305 obtained using COP+K is higher overall than with the PaPRIKa or Slovene approach
306 (predominantly Moderate). Only the map given by COP+K reveals the western sector of the
307 system as highly to very highly vulnerable to pollution.
308 Both the COP+K and PaPRIKa methods determine the swallow holes nearby the spring to entail
309 very high vulnerability (Figs. 6A and 6B), whereas the Slovene Approach method assigns them
310 a high vulnerability (Fig. 6C).
311 The three methods need to define an isochrone (24h, joining as many transit time data as
312 possible) to assess groundwater flow within the saturated zone, whether to estimate the t sub-
313 factor (COP+K and Slovene Approach methods) or to outline the isochrone for the I_{source}
314 parameter (PaPRIKa method). Only the source vulnerability map resulting from application of
315 the COP+K method shows the break line for isochrone 24h. While extrapolation techniques are

316 not appropriate in karst aquifers, yet necessary for vulnerability assessment, the errors should
317 be reduced by using as many transit time data as possible.
318 Regarding the importance of low permeability materials overlying the aquifer (when they do not
319 drain toward a swallow hole), divergent results are found. Both the COP method and Slovene
320 Approach classify such areas as having low vulnerability, whereas in the map obtained using
321 the PaPRIKa method these vulnerability classes are practically non-existent. In general, the
322 PaPRIKa method characterizes these areas as ones of moderate vulnerability.
323

324 **5.2. Validation**

325 Validation techniques were carried out to determine which of the three proposed maps for
326 vulnerability to pollution in the Villanueva del Rosario system would lead to the most consistent
327 results, using experimental techniques. The May 2011 multitracer test was specifically designed
328 for this purpose. Four tracers were injected simultaneously (details provided in section 3.2 and
329 Table 2). Figure 4 summarizes the injection points and groundwater flow paths deduced from
330 dye tracer tests performed in 2009 (pink) and 2011 (green).
331 Precipitation recorded on 2nd May was 45 mm (Fig. 3), preceded by moderate and continuous
332 rainfall events during the previous week amounting to 36 mm (April 25th to May 1st). The rainfall
333 infiltration led to an increase in outflow values of Villanueva del Rosario spring, from just 310 l/s
334 to 1,208 l/s in one day (Fig. 3). Only two tracers were detected: sulforhodamine-B and pyranine
335 (Tables 2 and 3).
336 In both cases, injection was facilitated by water runoff coming from adjacent surrounding areas,
337 draining toward the infiltration points. The main results of sample analyses in the laboratory and
338 field continuous monitoring are presented in Table 3.
339 Temporal distributions of breakthrough curves (Fig. 7), the lag-time of first detection (12h for
340 Sulforhodamine-B and 37h for Pyranine), as well as peak flow velocities (200 m/h for
341 Sulforhodamine-B and 134 m/h for Pyranine), are typical of aquifers with well-developed karstic
342 drainage, confirming the hydrogeological behaviour deduced from hydrodynamic and
343 hydrochemical analyses (Mudarra and Andreo, 2011). Moreover, values of transport parameters
344 characteristic of the system (average transit times, average effective flow velocity and
345 longitudinal dispersion coefficient), performed using a simple solute transport model for

346 Sulforhodamine-B and Pyranine breakthrough curves (Table 3), again reflect the existence of
347 preferential flows between the injection points and the discharge point (rapid infiltration through
348 karst conduits). Optimum values of these parameters were obtained by means of an automatic
349 method of optimization, using the computer modelling program of solute transport Trace 95
350 (Käss 1998). Thus, experimental results are consistent with output data from a previous tracer
351 test carried out in 2009 (Mudarra et al., 2010, 2014a).
352
353 **Table 3** Distances, discharge and statistical parameters deduced of the dye tracer test carried out in May
354 2011

Injection point	**P-4**	**P-1**
Dye tracer	Sulforhodamine-B	Pyranine
Injected mass (kg)	2	2
Distance to spring (m)	2810	6600
Time of first arrival (h)	12	37
Peak time (h)	14.1	49.2
Max. concentration (µg/l)	37.8	7.6
Peak velocity (m/h)	199.6	134.2
Discharge (l/s)	925	925
Recovery rate (%)	54.2	42.4
Average transit time (h)	15.1	49.5
Average effective flow velocity (m/h)	186.5	133.3
Longitudinal dispersion coef. (m^2/h)	3471.8	11475.4

355
356 The results given by the tracer test carried out in 2011 suggest that a hypothetical contaminant
357 spilled on the swallow hole (point P-1) quickly reached the Villanueva del Rosario spring due to
358 the high vulnerability. Moreover, dye injection over the well developed and uncovered
359 karrenfield (P-4) demonstrated that this karst landform, apparently without direct hydrological
360 connection with the saturated zone of the aquifer, could present vulnerability to pollution similar
361 to that of swallow holes. Furthermore, Villanueva del Rosario spring is more vulnerable to

362 pollution from karrenfield P-4 than to contamination from swallow hole P-1, as indicated by the
363 higher peak flow velocity of the former (Table 3).
364 The geological complexity of the aquifer (Fig. 2) and the heterogeneity of the karst medium
365 make it difficult to determine the reasons behind the non-detection of the other two fluorescent
366 dyes (uranine and eosin) in the Villanueva del Rosario spring, despite the long period recorded
367 by field spectrofluorometry (more than half a year) and the fact that all possible discharge points
368 were monitored. It may be that these substances —without any extra water from runoff, unlike
369 the other two cases— did not reach the drainage network within the karst system, being
370 retained within the soil matrix, or in stagnant zones or less permeable lithologies. The P-4 and
371 P-1 points received additional water runoff from adjacent areas for some hours after injection.
372 The additional water contributed to a more effective infiltration of the dye tracers spread at these
373 points.
374 Figure 8 provides zooms of the vulnerability maps (displayed in Fig. 6) in those zones where the
375 dye tracers were injected. This, together table 4, facilitates comparison of the vulnerability
376 classes obtained by each method with the experimental results. One main conclusion drawn
377 from the tracer tests is that the spring is very vulnerable to potential pollution from P-4
378 (maximum concentration at 14h), as well as to potential pollution from P-1, but to a lesser
379 degree (maximum value at 49h). Therefore, the map obtained by COP+K presents greater
380 consistency with the results derived from the injection and detection of dyes at the spring
381 (uranine and eosin in 2009, and pyranine and sulforhodamine-B in 2011).

Injection point	Dye tracer	Time of first arrival (h)	Peak velocity (m/h)	Vulnerability calculated / consistent with tracer test results		
				COP+K	Slovene Approach	PaPRIKa
P-3	Uranine	X		Moderate / -	Low / -	High / -
P-4	Sulforhodamine B	12	199.6	Very high /Yes	High / *	High / *
P-5	Eosin	X		High / -	Moderate / -	Moderate / -
P-1	Pyranine	37	134.2	High / Yes	High / Yes	High / Yes

* Uncertain. According to tracer test results, the spring Villanueva del Rosario is more vulnerable to any pollution from P-4 than P-1. Same vulnerability classes are not reasonable.

382 **Table 4** Summary table comparing tracers test results and vulnerability classes mapped

383 The non-detection of uranine and eosin in the spring water during the tracer test of May 2011
384 would mean that the vulnerability of P-3 and P-5 points is lower than in the areas where

pyranine and the sulforhodamine-B were injected (points P-1 and P-4). The map from the Slovene Approach is the only one showing this reduced (though somewhat varying) vulnerability for the two areas.

A main difference between the COP+K and Slovene Approach maps, on the one hand, and the PaPRIKa map on the other hand, lies in the vulnerability classes corresponding to low permeability rocks (Cretaceous marls) overlying the karst aquifer: Low or very low vulnerability classes are obtained with the two first methods. No experimental results confirm the protective capacity of the marls, that is, when no runoff flows into a swallow hole or toward an area of concentrated infiltration. Still, the regional hydrogeological background and field validation work by Perrin et al. (2004) suggest that such lithology increases the natural protective capacity of an aquifer against pollutant substances, in contrast with the PaPRIKA results (Figs. 6B and 8).

5.3. Protection zoning

The protection zoning of the catchment area of Villanueva del Rosario spring, displayed in Fig. 9, is the result of transforming source vulnerability classes into protection zones according to the methodological proposal presented in section 4 and Figure 5.

The validation results demonstrate that the most successful method for source vulnerability mapping is COP+K. Even though the three methods incur in error, the COP+K map generally shows high vulnerability for the western sector of the aquifer, while the vulnerability classes assigned to dye injection points are consistent with the achieved results. Thus, following the Andreo et al. (2009) recommendations as well as considerations mentioned in section 4, conversion rules from vulnerability value to degree of protection are shown in table 5.

COP+K value	Source vulnerability classes	Protection zones
1-2	High	Zone I
3	Moderate	Zone II
≥ 4	Low	Zone III

Table 5 Conversion rules from source vulnerability classes to protection zones

Through the application of the Table 5 breakdown at source vulnerability maps, protection zones could be discerned within the Villanueva del Rosario catchment area (Fig. 9):

1. Zone I, which requires high protection. It coincides with the areas of high source vulnerability, corresponding to very high resource vulnerability (swallow hole catchment areas, karst features with high infiltration capacity, some flat limestone outcrops) and, additionally, the areas having high resource vulnerability and a transit time lower than 1 day.

2. Zone 2 comprises areas that require moderate protection, formed by carbonate outcrops not included in Zone I. In general, these are the sectors with moderate source vulnerability: that is, moderate resource vulnerability and transit time lower than 1 day, or with high resource vulnerability and higher flow transit times.

3. Zone 3, requiring a lower degree of protection: small patches restricted to areas where low permeability rocks overlie the aquifers (Cretaceous marls, Flysch clays, silty soils over 50 cm thick). Additionally, areas having moderate resource vulnerability and transit times higher than 1 day are included in this class.

6. Discussion

The vulnerability maps illustrating the susceptibility to contamination of the Villanueva del Rosario spring differ significantly depending on the applied method, although all were obtained using methods specially developed for karst aquifers, based on the same data sources and applied by the same researcher. This controversial aspect, as reported previously (Vías et al., 2005; Neukum and Hötzl, 2007; Ravbar and Goldscheider, 2009; Marín et al., 2012, 2014), highlights the need for such maps to be validated. This stands as an essential requirement for any assessment of vulnerability to contamination, in order that effective groundwater protection and management of groundwater resources may be achieved.

In general, the three methods applied here classify the carbonate outcrops in ranges of low to very high degrees of contamination vulnerability. The differing classes depend on the nature of the carbonate rocks (limestones or dolostones) of the aquifer matrix, the thickness of the unsaturated zone, the abundance of karst landforms and their effect on water infiltration, the slope (particularly significant for PaPRIKa method, as underlined by Marín et al., 2012), and finally, the transit time.

At any rate, results cannot be immediately assumed to be accurate; rather, the validation of vulnerability maps and protection zoning is essential for proper land-use planning.

Validation may be done on the basis of hydrodynamic and hydrochemical responses of the main springs, jointly with the temporal evolution of natural tracers of infiltration, and complemented by dye tracer tests that are specifically designed to check the vulnerability to pollution. The joint use of natural and dye tracer is not very common in karst hydrogeology (Auckenthaler et al., 2002; Einsiedl, 2005; Pronk et al., 2009; Ravbar et al., 2012; Mudarra et al., 2014b), and even less so for validating maps of vulnerability to contamination (Perrin et al., 2004; Marín et al., 2012). Yet because natural and artificial tracers complement each other, their joint use can enhance our understanding of karst aquifer processes (infiltration, recharge and vulnerability), as noted by Marín and Andreo (2015). This also means that the injection sites must be carefully selected, taking into account the hydrological conditions under which the tracer tests are performed, while adequately sampling and monitoring routines. Indeed, these are fundamental aspects involved in achieving reliable, sustainable results.

During the 2009 tracer test in the pilot site, a detailed monitoring of natural responses, environmental tracers (TOC and intrinsic fluorescence) and artificial dye tracers in the water drained by the Villanueva del Rosario spring reflected the existence of highly developed karst conduits in this sector of the aquifer, with fast flows and very short transit times for water within the system (less than one day, Mudarra and Andreo, 2011 and Mudarra et al., 2014a). However, maximum values of natural soil tracers (and minimum of EC) were recorded in the spring water before the dye tracers were detected, which was interpreted as a signal that the global system response (including diffuse infiltration) was even faster and more sensitive than that produced from infiltration concentrated at a single point on the surface (local recharge). This is coherent with the high and very high vulnerability classes determined for the western catchment area of Villanueva del Rosario spring (Fig. 6A). Accordingly, this area requires high protection (zone I in Fig. 9).

In the case of the 2011 experiment, no data about environmental tracers is available; only the dye tracer results expounded in section 5.2 serve to validate the vulnerability maps. Still, of breakthrough curve morphologies for pyranine, and especially for sulforhodamine-B (Fig. 7), are similar to those recorded in 2009 for eosin and uranine, thus indicating fast flow transit from the injection areas (localized recharge) to the spring. Bearing in mind the slightly different hydrodynamic conditions of the two experiments (2009: very high water condition; 2011: high-

intermediate), the findings of the first one, in terms of natural tracer infiltration, could be extrapolated to the 2011 tracer test in order to validate the corresponding vulnerability map.

In light of studies of the natural responses (hydrodynamic and hydrochemical, mainly TOC and intrinsic fluorescence) of the Villanueva del Rosario spring water previously published by Mudarra et al. (2011 and 2014b), there would be a high vulnerability overall of the water supply to hypothetical pollution.

The non-detection of uranine and eosin tracers (which did not reach the springs in the 2011 test) suggests that the vulnerability of P-3 and P-5 points (Fig. 8) is lower than in the areas where pyranine and sulforhodamine-B were injected (points P-1 and P-4). Nevertheless, it is necessary to carry out further research in these areas, including new tracer tests, to corroborate the vulnerability class of these particular sectors of the aquifer.

The Villanueva del Rosario protection zones obtained by the COP+K method (Fig. 9) are coherent with the present body of knowledge concerning hydrogeology and the applied validation techniques. In general, areas with outcrops of carbonate rocks are categorized as zones I or II, depending on their carbonate nature, distance to the spring, degree of karstification and preferential infiltration features. On the other hand, the lowest degrees of protection are required in zones where impermeable materials (soils or marly and clay lithologies) overlie the aquifer, and they do not drain toward swallow holes.

7. Conclusions

An approach for protection zoning has been proposed based on source vulnerability mapping obtained by the COP+K method. The source vulnerability map was transformed into protection zoning, then validated with dye tracer tests. Thus, the proposed approach constitutes a more reliable and effective procedure for protecting karst spring water systems.

The source vulnerability map obtained by applying COP+K is more consistent than the hydrogeologic research results derived using other approaches at the pilot site of Villanueva del Rosario. However, this method displays a breaking line in high and moderate vulnerability classes resulting from the extrapolation of transit time data. Such errors due to extrapolation should be reduced by gathering more flow velocity data.

499 The delineation of protection zones around karst aquifers used for water supply is a
500 manageable process, calling for source vulnerability mapping in addition to hydrogeological
501 studies. The procedure proposed in this paper is meant to complement protection zone
502 mapping, particularly in countries lacking guidelines for protecting the water resources of karst
503 aquifers.
504 A multitracer test conducted in 2011, designed *ad hoc* to validate the vulnerability maps,
505 corroborates that aquifer sectors influenced by well-developed exokarst features could be even
506 as vulnerable to pollution as sinkholes, extremely vulnerable. It should be noted that at two of
507 the four points in the catchment area of Villanueva del Rosario spring where the vulnerability
508 was estimated experimentally (by the injection of dye tracers), the methods did not provide
509 reliable maps.
510 Despite the importance of mapping validation in the context of groundwater protection and
511 management, this phase is bypassed in many cases, considered optional or superfluous. Yet
512 because the final goal of the entire methodological process is to implement groundwater
513 protection mapping (i.e. protective zoning around abstraction points) as part of effective land-
514 use planning, the implementation of a non-validated map could trigger problems associated with
515 incorrect perimeter zoning and/or land-use management. Therefore, the protection of karst
516 water sources should be based on four pillars: (i) hydrogeological studies, (ii) source
517 contamination vulnerability assessment, (iii) validation of vulnerability mapping, and (iv)
518 implementation in land-use planning.
519
520 ***Acknowledgements*** This work is a contribution to projects CGL2012-32590 of DGICYT and
521 IGCP 598 of UNESCO, and to Research Group RNM-308 funded by the Autonomous
522 Government of Andalusia (Spain). The authors thank four anonymous reviewers for their
523 constructive criticism which contributed to improving the original version of the manuscript, and
524 to Jean Sanders for his English revision.
525

526 **References**

527 Adams, B., Foster, S.D., 1992. Land-surface zoning for groundwater protection. Journal of the
528 Institution of Water and Environmental Management 6(3), 312-320.

529 Andreo, B., Ravbar, N., Vías, J.M., 2009. Source vulnerability mapping in carbonate (karst)
530 aquifers by extension of the COP method: application to pilot sites. Hydrogeol. J. 17(3), 749–
531 758. DOI 10.1007/s10040-008-0391-1.
532 Andreo, B., Goldscheider, N., Vadillo, I., Vías, J.M., Neukum, C., Sinreich, M., Jiménez, P.,
533 Brechenmacher, J., Carrasco, F., Hötz, H., Perles, M.J., Zwahlen, F., 2006. Karst groundwater
534 protection: First application of a Pan-European Approach to vulnerability, hazard and risk
535 mapping in the Sierra de Líbar (Southern Spain). Sci. Total Environ. 357(1-3), 54-73.
536 Auckenthaler, A., Raso, G., Huggenberger, P., 2002. Particle transport in a karst aquifer: natural
537 and artificial tracer experiments with bacteria, bacteriophages and microspheres. Water Sci.
538 Technol. 46(3), 131–138.
539 Benischke, R., Goldscheider, N., Smart, C., 2007. Tracer techniques. In: Goldscheider, N.,
540 Drew, D. (Eds), Methods in Karst Hydrogeology, Taylor & Francis, London, pp. 147-170.
541 Daly, D., Dassargues, A., Drew, D., Dunne, S., Goldscheider, N., Neale, S., Popescu, C.,
542 Zwhalen, F., 2002. Main concepts of the “European Approach” for (karst) groundwater
543 vulnerability assessment and mapping. Hydrogeol. J. 10(2), 340–345
544 Davis, A.D., Long, A.J., Wireman, M., 2002. KARSTIC: a sensitive method for carbonate
545 aquifers in karst terrain. Environ. Geol. 42, 65–72.
546 DELG-EPAGS, D., 1999. A scheme for the protection groundwater. Department of Environment
547 and Local Government, Environmental Protection Agency and Geological Survey of Ireland,
548 Dublin.
549 Dörfliger, N., Zwahlen, F., 1997. EPIK: a new method for outlining of protection areas in karstic
550 environments. In: Günay G., Johnson I. (Eds.), Proceedings 5th International symposium and
551 field seminar on karst waters and environmental impacts. Antalya, Sep. 1995, Balkema,
552 Rotterdam, pp. 117–123.
553 Dörfliger, N., Plagnes, V., 2009. Cartographie de la vulnérabilité des aquifères karstiques guide
554 méthodologique de la méthode PaPRIKa [Mapping the vulnerability of karst aquifers. Guidelines
555 of the method PAPRIKa]. Rapport BRGM RP-57527-FR, BRGM, Orleans, France.

556 DVGW, 2006. Richtlinien für Trinkwasserschutzgebiete, Part 1: Schutzgebiete für Grundwasser.
557 Deutscher Verein des Gas- undWasserfaches DVGW-Regelwerk. Working Paper W 101,
558 Eschborn.

559 Einsiedl, F., 2005. Flow system dynamics and water storage of a fissured-porous karst aquifer
560 characterized by artificial and environmental tracers. J. Hydrol. 312, 312–321. DOI:
561 10.1016/j.jhydrol.2005.03.031.

562 European Commission, 2000. Directive 2000/60/EC of the European Parliament and of the
563 Council of 23rd October 2000 establishing a framework for Community action in the field of
564 water policy, Official Journal 22 December 2000 L 327/1, European Commission, Brussels.

565 European Commission, 2007. Common implementation strategy for the Water Framework
566 Directive (200/60/EC). Guidance Document nº 16 on Groundwater in Drinking Water Protected
567 Areas. European Commission, Brussels.

568 European Commission, 1995. Hydrogeological aspects of groundwater protection in karstic
569 areas. Report EUR 16547 EN, Brussels

570 European Commission, 1991. Council Directive 91/676/EEC of 12 December 1991 concerning
571 the protection of waters against pollution caused by nitrates from agricultural sources.
572 OJL375:0001–0008, 31/12/1991

573 Ford, D.C., Williams, P.W., 1989. Karst geomorphology and hydrology. Chapman and Hall.

574 Foster, S., 1987. Fundamental concepts in aquifer vulnerability, pollution risk and protection
575 strategy. In: Van Duijvenbooden, W., Van Waegeningh, H.G. (Eds.), Vulnerability of soil and
576 groundwater to pollutants 38, 69-86. TNO Committee on hydrological research.

577 Foster, S., Hirata, R., Andreo, B., 2013. The aquifer pollution vulnerability concept: aid or
578 impediment in promoting groundwater protection? Hydrogeol. J. 21, 1389–1392. DOI
579 10.1007/s10040-013-1019-7.

580 Goldscheider, N., 2010. Delineation of spring protection zones. In: Kresic, N. and Stevanovic, Z.
581 (Eds.), Groundwater Hydrology of Springs, pp. 305 - 338. DOI: 10.1016/B978-1-85617-502-
582 9.00008-6.

583 Goldscheider, N. 2008. A new quantitative interpretation of the long-tail and plateau-like
584 breakthrough curves from tracer tests in the artesian karst aquifer of Stuttgart, Germany.
585 Hydrogeol. J. 16(7), 1311-1317. DOI: 10.1007/s10040-008-0307-0.

586 Goldscheider, N., Hötzl, H., Fries, W., Jordan, P., 2001. Validation of a vulnerability map (EPIK)
587 with tracer tests. In: Mudry, J., Zwahlen, F. (Eds.), 7th Conference on Limestone Hydrology and
588 Fissured Media, Besançon, France, 20–22 September 2001, University de Franche-Comté,
589 Besançon, pp 167–170.

590 Goldscheider, N., Klute, M., Sturm, S., Hötzl, H., 2000. The PI method - a GIS -based approach
591 to mapping groundwater vulnerability with special consideration of karst aquifers. Z. Angew.
592 Geol. 46(3), 157-166.

593 Hartmann, A., Mudarra, M., Andreo, B., Marín, A.I., Wagener, T., Lange, J., 2014. Identifying
594 spatio-temporal impacts of hydro-climatic extremes on a karst aquifer by a GIS-based recharge
595 estimation method and a lumped karst simulation model. Water Resour. Res., 50(8), 6507-
596 6521. DOI:10.1002/2014WR015685.

597 Jeannin, P.Y., Eichenberger, U., Sinreich, M., Vouillamoz, J., Malard, A., Weber, E., 2013.
598 KARSYS: a pragmatic approach to karst hydrogeological system conceptualisation.
599 Assessment of groundwater reserves and resources in Switzerland. Environ. Earth Sci. 69,
600 999–1013. DOI: 10.1007/s12665-012-1983-6.

601 Käss, W., 1998. Tracing Technique in Geohydrology. Balkema, Rotterdam. 600 pp.

602 Kavouri, K., Plagnes, V., Tremoulet, J., Dörfliger, N., Fayçal, R., Marchet, P., 2011. PaPRIKa: a
603 method for estimating karst resource and source vulnerability – application to the Ouysse karst
604 system (southwest France). Hydrogeol. J. 19 (2), 339-353. DOI: 10.1007/s10040-010-0688-8.

605 Margat, J., 1968. Vulnerabilité des nappes d'eau souterraine á la pollution. Bases de la
606 cartographie. Doc. 68 sgl 198 hyd, BRGM, Orléans.

607 Marín, A.I., Andreo, B., 2015. Vulnerability to Contamination of Karst Aquifers. In: Z. Stevanović
608 (Ed.), Karst Aquifers – Characterization and Engineering, Professional Practice in Earth
609 Sciences, DOI 10.1007/978-3-319-12850-4_8

610 Marín, A.I., Ravbar, N., Kovačič, G., Andreo, B., Petrič, M., 2014. Application of Methods for
611 Resource and Source Vulnerability Mapping in the Orehek Karst Aquifer, SW Slovenia. In:
612 Mudry, J., Zwahlen, F., Bertrand, C., LaMoreaux, J.W. (Eds.), H2Karst Research in Limestone
613 Hydrogeology. Environ. Earth Sci. pp. 139-150. DOI: 10.1007/978-3-319-06139-9_10.

614 Marín, A.I., Dörfliger, N., Andreo, B., 2012. Comparative application of two methods (COP and
615 PaPRIKa) for groundwater vulnerability mapping in Mediterranean karst aquifers (France and
616 Spain). Environ. Earth Sci. 65(8), 2407-2421. DOI: 10.1007/s12665-011-1056-2.

617 Martín-Algarra, M., 1987. Evolución geológica alpina del contacto entre las Zonas Internas y
618 Externas de la Cordillera Bética. Ph.D. Thesis, University of Granada, Spain, 1171 pp.

619 Mudarra, M., Andreo, B., 2011. Relative importance of the saturated and the unsaturated zones
620 in the hydrogeological functioning of karst aquifers: The case of Alta Cadena (Southern Spain).
621 J. Hydrol. 397(3-4), 263-280. DOI: 10.1016/j.jhydrol.2010.12.005.

622 Mudarra, M., Andreo, B., Marín, A.I., Vadillo, I., Barberá, J.A., 2014a. Combined use of natural
623 and artificial tracers to know the hydrogeological functioning of a karst aquifer: the Villanueva
624 del Rosario system (Andalusia, southern Spain). Hydrogeol. J. 22(5), 1027-1039. DOI:
625 10.1007/s10040-014-1117-1.

626 Mudarra, M., Andreo, B., Barberá, J.A., Mudry J., 2014b. Hydrochemical dynamics of TOC and
627 NO_3^- contents as natural tracers of infiltration in karst aquifers. Environ. Earth Sci. 71, 507-523.
628 DOI: 10.1007/s12665-013-2593-7.

629 Mudarra, M., Andreo, B., Baker, A., 2011. Characterisation of dissolved organic matter in karst
630 spring waters using intrinsic fluorescence: Relationship with infiltration processes. Sci. Total
631 Environ. 409(18), 3448 - 3462. DOI:10.1016/j.scitotenv.2011.05.026.

632 Mudarra, M., Marín, A.I., Andreo, B., Vadillo, I., Barberá, J.A., Neukum, C., Sánchez-García, D.,
633 Liñán, C., Pérez-Ramos, I., 2010. Investigación del funcionamiento hidrogeológico del acuífero
634 carbonatado drenado por el manantial de Villanueva del Rosario (Alta Cadena, Málaga) a partir
635 de un ensayo de trazadores. Geogaceta 48, 131–134.

636 Neukum, C., Hötzl, H., 2007. Standardization of vulnerability maps. Environ. Geol, 51(5), 689-
637 694. DOI: 10.1007/s00254-006-0380-4.

638 Perrin, J., Pochon, A., Jeannin, P., Zwahlen, F., 2004. Vulnerability assessment in karstic areas:
639 validation by field experiments. Environ. Geol. 46, 237-245. DOI: 10.1007/s00254-004-0986-3.

640 Peyre, Y., 1974. Géologie d'Antequera et de sa région (Cordillères Bétiques, Espagne). PhD
641 Thesis, University of Paris, Inst. Nat. Agronomique, Paris, France.

642 Pronk, M., Goldscheider, N., Zopfi, J., Zwahlen, F., 2009. Percolation and particle transport in
643 the unsaturated zone of a karst aquifer. Ground Water 47(3), 361–369. DOI:10.1111/j.1745-
644 6584.2008.00509.x.

645 Turk, J., Malard, A., Jeannin, P.Y.; Petrič, M., Gabrovšek, , F., Ravbar, N., Vouillamoz, J.,
646 Slabe, T., Sordet, V., 2014. Hydrogeological characterization of groundwater storage and
647 drainage in an alpine karst aquifer (the Kanin massif, Julian Alps). Hydrol.Process. DOI:
648 10.1002/hyp.10313.

649 Ravbar, N., Goldscheider, N., 2009. Comparative application of four methods of groundwater
650 vulnerability mapping in a Slovene karst catchment. Hydrogeol. J., 17(3), 725-733. DOI:
651 10.1007/s10040-008-0368-0.

652 Ravbar, N., Barberá, J.A., Petrič, M., Kogovsěk, J., Andreo, B., 2012. The study of
653 hydrodynamic behaviour of a complex karst system under low-flow conditions using natural and
654 artificial tracers (the catchment of the Unica River, SW Slovenia). Environ. Earth Sci. 65, 2259–
655 2272. DOI: 10.1007/s12665-012-1523-4.

656 Ravbar, N., Goldscheider, N., 2007. Proposed methodology of vulnerability and contamination
657 risk mapping for the protection of karst aquifers in Slovenia. Acta Carsologica, 36(3), 461-475.

658 SAEFL, S., 2004. Wegleitung Grundwasserschutz [Practical guide: groundwater protection].
659 Swiss Agency for the Environment, Forests and Landscape, Bern.

660 Vías, J., Andreo, B., Perles, M., Carrasco, F., Vadillo, I., Jiménez, P., 2006. Proposed method
661 for groundwater vulnerability mapping in carbonate (karstic) aquifers: the COP method.
662 Hydrogeol. J. 14(6), 912-925. DOI: 0.1007/s10040-006-0023-6.

663 Vías, J.M., Andreo, B., Perles, M.J., Carrasco, F., 2005. A comparative study of four schemes
664 for groundwater vulnerability mapping in a diffuse flow carbonate aquifer under Mediterranean
665 climatic conditions. Environ. Geol. 47(4), 586-595. DOI: 10.1007/s00254-004-1185-y.

Zaporozec, A., 1994. Guidebook on mapping groundwater vulnerability, 16, Concept of groundwater vulnerability: 3-8. International Contributions to Hydrogeology, Verlag Heinz Heise, Hannover. 308 pp.

Zwahlen, F. ed., 2004. Vulnerability and risk mapping for the protection of carbonate (Karstic) aquifers. Final report COST Action 620. EUR 20912. European Commission, Directorate-General for Research, Brüssel, Luxemburg. 297 pp.

Figure captions

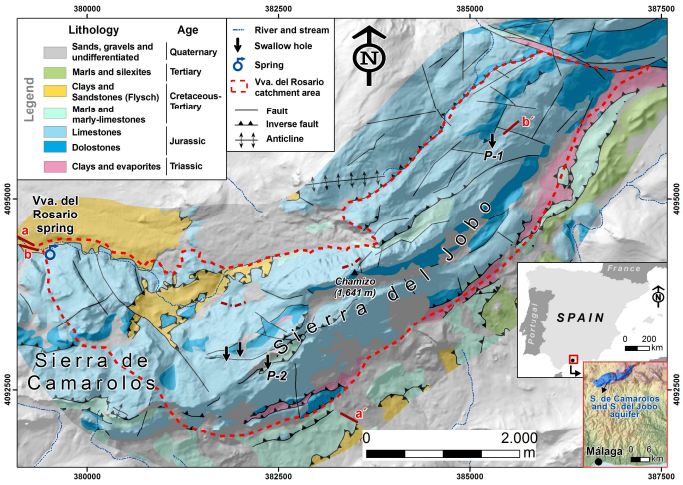

Fig. 1 Location and geological map of the catchment area of Villanueva del Rosario spring (and adjacent area).

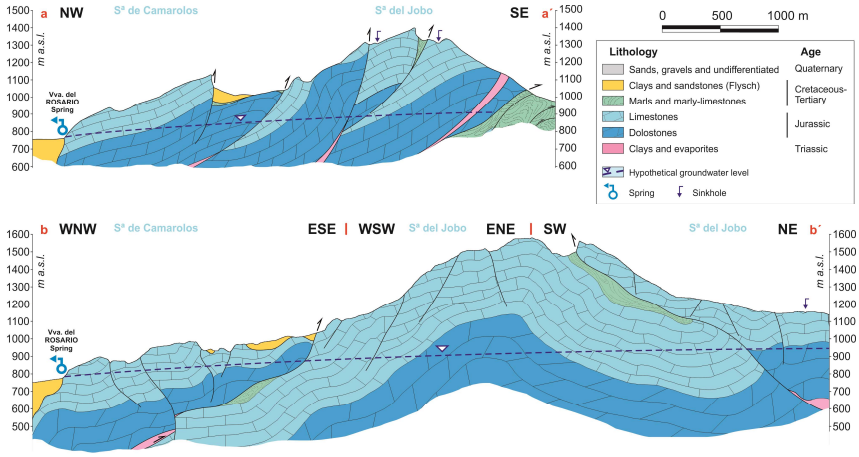

Fig. 2 Geological-hydrogeological cross-sections of Villanueva del Rosario aquifer (Mudarra et al., 2014a) See location in Figure 1.

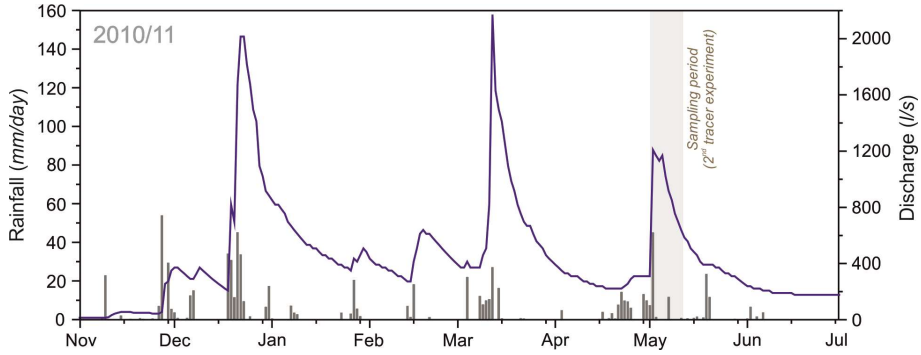

680

681 **Fig. 3** Daily hydrograph of Villanueva del Rosario spring versus precipitation from November

682 2010 to July 2011.

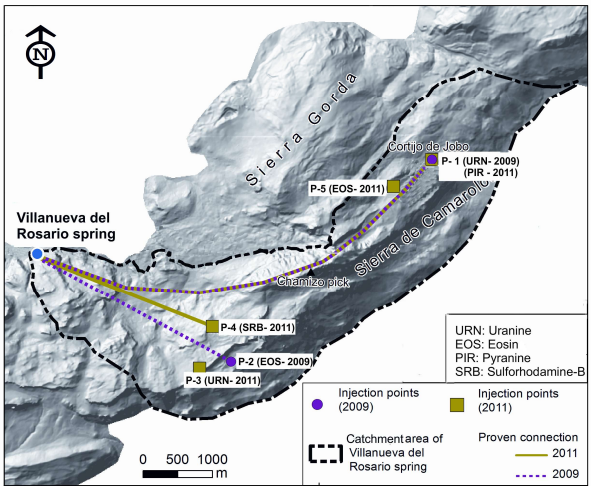

683

684 **Fig. 4** Injection points and groundwater flow paths deduced from dye tracer tests carried out in

685 2009 (pink) and 2011 (green). More details in Tables 2 and 3.

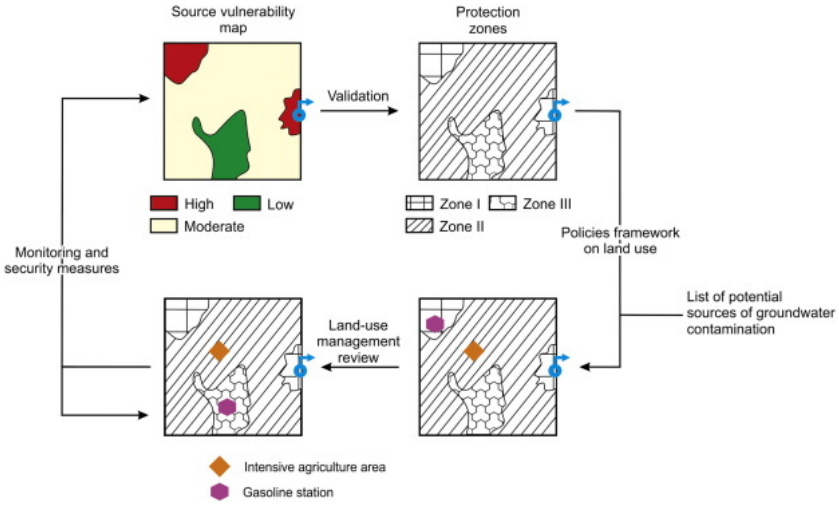

686

687 **Fig. 5** Sketch of the implementation steps for protection zoning of sources (springs and wells)

688 for water supply proposed in this work.

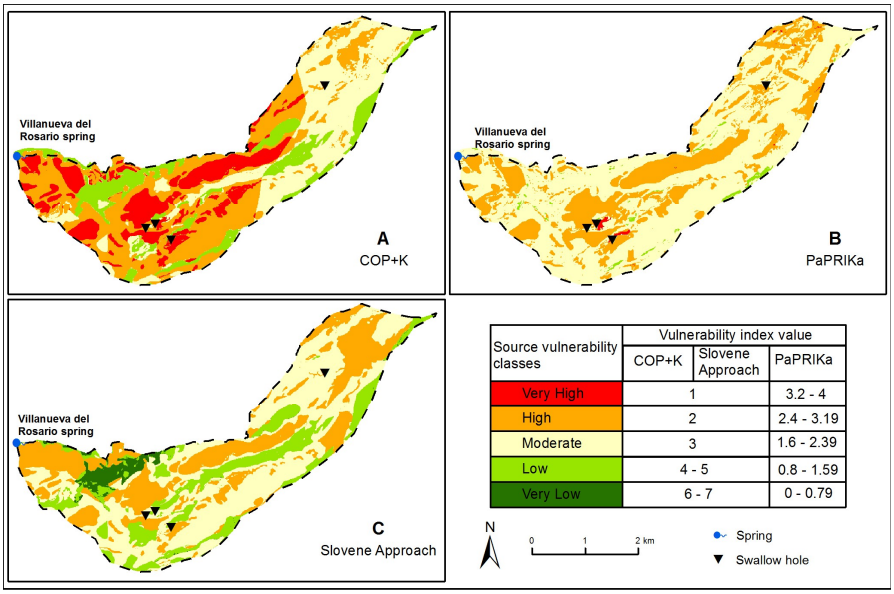

689

690 **Fig. 6** Source vulnerability maps of Villanueva del Rosario karst spring (A, COP+K method; B,

691 PaPRIKa method; C, Slovene Approach).

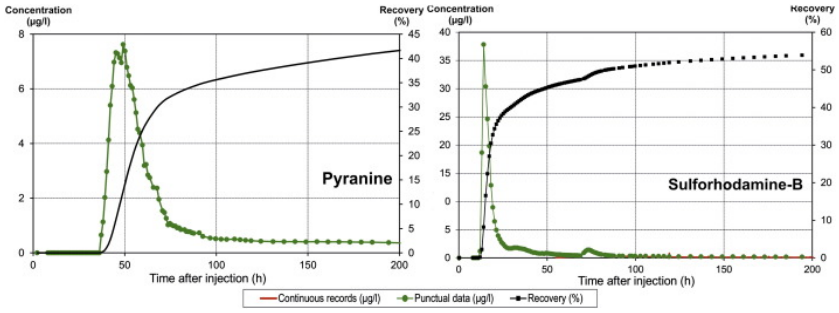

692

693 **Fig. 7** Pyranine (left) and sulforhodamine-B (right) breakthrough curves recorded at the

694 Villanueva del Rosario spring during the dye tracer test on May 2011.

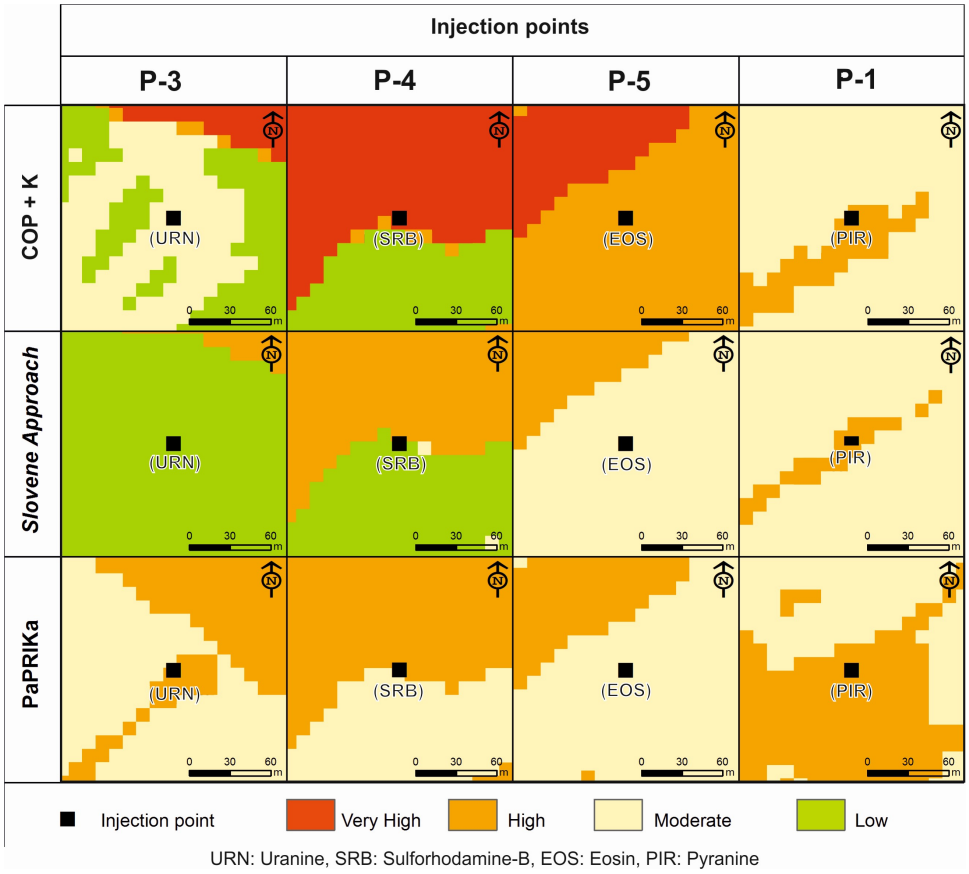

Fig. 8 Contamination vulnerability after COP+K, Slovene Approach and PaPRIKa methods on the injection points where the tracer dyes were injected on May 2011.

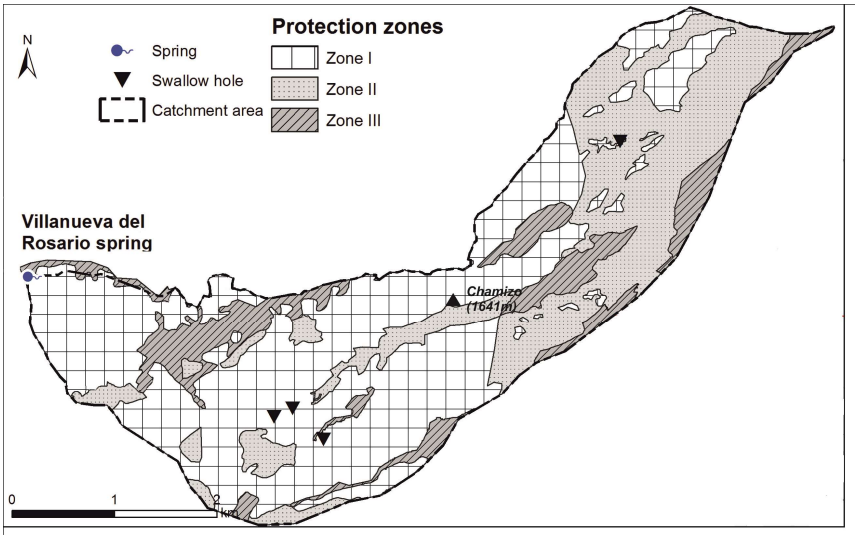

Fig. 9 Proposal for protection zoning for Villanueva del Rosario spring, according to COP+K method.